Taylor & Francis
Taylor & Francis Group

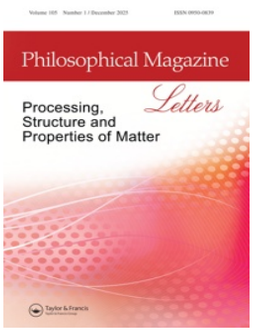

Philosophical Magazine Letters

ISSN: 0950-0839 (Print) 1362-3036 (Online) Journal homepage: www.tandfonline.com/journals/tphl20

Extraordinary enhancement of the toughness and plasticity of multilayered metallic glass composites with gradient heterogeneous interfaces

Yongwei Wang, Guangping Zheng & Mo Li

To cite this article: Yongwei Wang, Guangping Zheng & Mo Li (2025) Extraordinary enhancement of the toughness and plasticity of multilayered metallic glass composites with gradient heterogeneous interfaces, Philosophical Magazine Letters, 105:1, 2544113, DOI: 10.1080/09500839.2025.2544113

To link to this article: https://doi.org/10.1080/09500839.2025.2544113

Published online: 22 Aug 2025.

PHILOSOPHICAL MAGAZINE LETTERS
2025, VOL. 105, NO. 1, 2544113
https://doi.org/10.1080/09500839.2025.2544113

Extraordinary enhancement of the toughness and plasticity of multilayered metallic glass composites with gradient heterogeneous interfaces

Yongwei Wang[a], Guangping Zheng[b] and Mo Li[c]

[a]Collaborative Innovation Center of Steel Technology, University of Science and Technology Beijing, Beijing, People's Republic of China; [b]Department of Mechanical Engineering, Hong Kong Polytechnic University, Kowloon, Hong Kong, People's Republic of China; [c]School of Materials Science and Engineering, Georgia Institute of Technology, Atlanta, GA, USA

ABSTRACT

A strategy is proposed to enhance the mechanical properties of metallic glasses using multilayered composites with various initial free-volume gradient interfaces and validated by finite element modelling. We found that the ductility of the composites improves significantly with the increasing number of layers. The main factors and the underlying mechanisms are (a) the *gradient interface* with varying free volume densities that can reduce the local stress concentration, (b) *size effects* imposed by the layer thickness that limits the local shear and shear bands to grow critically longer and thicker to cause catastrophic failure, (c) the presence of interface barriers to increase the *probability of blocking and retarding* the shear banding, and (d) the *heterogeneity introduced by the statistical distribution of free volumes*. The results demonstrate that the multilayered composites are promising in solving the strength-ductility tradeoff in metallic glasses.

ARTICLE HISTORY
Received 4 April 2025
Accepted 1 August 2025

KEYWORDS
Multilayered metallic glass composite; free volume theory; shear band; toughness

1. Introduction

Since their invention, metallic glasses (MGs) [1] have attracted tremendous research interest due to their unique properties, such as high specific strength, good corrosion resistance, soft magnetic properties and net-shape formability [2–5]. However, the plastic deformation of MGs is highly localized within narrow regions called shear bands (SBs), resulting in catastrophic failure and limiting the structural reliability and their applications [6–9]. Enormous efforts have been made in recent years to improve the plasticity of MGs. Under compression, some MGs exhibit large plasticity [4–16]. However, under tensile deformation, extended room temperature plasticity for MGs is still scarce. The concept of the heterogeneous structure, including composite, is widely recognized to improve the plasticity of MGs by blocking the SBs [4,17,18]. For instance, introduction of the second phases or inclusions, surface treatments or mechanical deformations, such as shot peening or grinding in the surface region, can induce structural or chemical heterogeneity that can improve ductility [8–16,19,20]. It is revealed in a theoretical model that the statistical distribution and spatial inhomogeneity [21,22], especially the *gradient* of free volumes (FVs) at the interfaces between the inclusions and the MG matrix, affect significantly the mechanical properties of MGs [23]. The strength and toughness are enhanced with increasing free-volume gradient at interfaces by blocking the main SBs, which initiate from the softer regions with high concentrations of FVs and propagate to the harder regions with low free-volume concentrations [24,25]. The model system is made of a single interface, rather limited in revealing the potential of changing the shear banding behaviour. A natural extension of this mechanism is to build many layers of different MGs with FV gradient interfaces such that the SBs can be blocked multiple times when crossing the interfaces, which is expected to lead to exceptional ductility. Experiments demonstrated that a multilayer strategy could lead to the enhancement of the mechanical

CONTACT Yongwei Wang yw_wang@ustb.edu.cn Collaborative Innovation Center of Steel Technology, University of Science and Technology Beijing, Beijing 100083, People's Republic of China and Mo Li mo.li@gatech.edu School of Materials Science and Engineering, Georgia Institute of Technology, Atlanta, GA 30332, USA

properties of MGs and their composites [26–35]. The amorphous/amorphous and crystalline/amorphous nanolaminate samples fabricated by magnetron sputter deposition [33–35] and the multilayer-based bulk metallic glasses synthesized by thermoplastic bonding [27] exhibit enhanced plasticity. In the crystalline/amorphous nanolaminates, the SBs formed in the MG layers are blocked at the crystal-amorphous interfaces, and subsequent deformation (and plasticity) of the composites shows substantially enhanced plasticity contributed by dislocations initiated in the crystalline layers [35]. For amorphous-amorphous interfaces, due to the disordered atomic structure, we are limited in directly observing the defect formation, such as in the crystalline layers [35] or deformation mechanisms, although an obvious enhancement in strength and toughness has been found. This limitation motivates us to carry out the theoretical modelling here.

2. Methods and sample preparation

In the present work, we focus on exploring the underlying mechanisms of multilayered MG composites using theoretical modelling, so we can examine the key factors in the model systems. Using finite element modelling (FEM), we can obtain the mechanical properties of multilayered MG composites with various initial FV gradient interfaces to investigate the influence of the layered structures on their mechanical properties quantitatively and the mechanisms of shear banding across the multiple FV-gradient interfaces. The choice of using FEM is deliberate because it allows us to reach the length and time scale accessible in experiment, so a comparison between the theoretical and experimental results could be made in the future.

FV gradient is defined as the steepness of the variation of FV density in space. This spatial heterogeneity introduces changes in local mechanical properties. The MG with low FV density is stronger, and the one with high FV density is softer. Operationally, in the FEM, we first assign the FV values that can be drawn from the *statistical distributions,* by the transformation relation or beta distribution, 0.04Beta(x; a, b) + 0.03, where a and b are parameters and $0 < x < 1$ is the free volume density. The range of the free volume density in our case is from 0.03 to 0.07, with a mean of 0.05. When a equals b, the beta statistical distribution is symmetric. When $a = 0.1$ or $a = 1$, we have the symmetrical bimodal or random distributions respectively. Then we vary the FV values drawn from the distribution at the mesh points at different locations, according to certain *spatial distributions* to create an FV *gradient*. The FV gradient in the interface region connects two adjacent MGs with different FV densities. Our previous works [21–23] showed that the variance or dispersity of FV from the statistical distribution has unusual effects on leveraging the plasticity of MGs: The MG with bimodal FV distribution exhibits enhanced toughness and even strain hardening behaviour than those with random FV distribution, and the strength and toughness improve further with increasing FV gradient [23], exhibiting unusual *FV gradient effect*. In this work, we further explore the influence of the FV-gradient interfaces on mechanical properties in multilayered MG composites (see Figure 1) in light of the recent theoretical work on gradient interface [23] and the experimental works mentioned above [26–35].

The constitutive models that incorporate explicitly the FV variations in MGs [21–24,36–38] are used in the FEM. Since technical details are available already in Ref. [21,22,24], here we only briefly describe the methods: We first create several multilayered MG composites with different FV density gradients, as shown in Figure 1, along with the MG samples without the gradient as a comparison. To obtain the mechanical properties from the samples, we use an elasto-plastic constitutive model that incorporates FV as an internal state variable. The deformation strain in this model includes an elastic and a plastic part, $\varepsilon_{ij} = \varepsilon_{ij}^{el} + \varepsilon_{ij}^{pl}$, where ε_{ij}^{el} is the elastic strain. We obtain the plastic strain from the plastic flow equation $d\varepsilon_{ij}^{pl} = d\lambda \dfrac{\partial g}{\partial \sigma_{ij}}$, where g is the plastic potential function, $g(\sigma_{ij}) = b' I_1 + \sqrt{3J_2} - K$, λ is the plastic deformation parameter related to free volume change, σ_{ij} is the Cauchy stress and I_1 is the first invariant of the stress tensor σ_{ij} and J_2 is the second invariant of the deviatoric stress. The effective stress and increment of equivalent plastic strain are obtained through the relations $\sigma_{DP} = a' I_1 + \sqrt{3J_2}$ and $d\varepsilon_{eff}^{pl} = \sqrt{2/3 d\varepsilon_{ij}^{pl} d\varepsilon_{ij}^{pl}}$, where a', b' and K are constants where $a' = b'$ for the associated flow rule. The plastic strain is a function of the free volume production by the following relation $\dot{\varepsilon}_{eff}^{pl} = 2f \exp\left(-\frac{\alpha v^*}{\bar{v}_f}\right) \exp\left(-\dfrac{\Delta G^m}{k_B T}\right) \sinh\left(\dfrac{\tau \Omega}{2 k_B T}\right)$

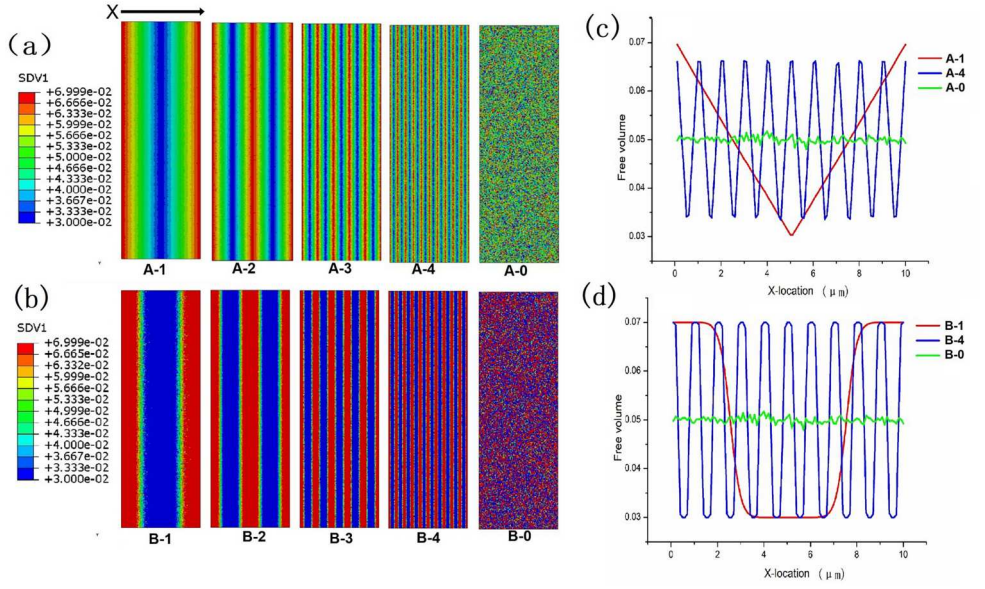

Figure 1. The initial free volume distribution in space drawn from the statistical distribution (a beta function) for the systems (A-1, A-2, A-3 and A-4) with uniform FV distribution (beta (1,1) ×0.04+0.03, Case A) (a) and systems (B-1, B-2, B-3 and B-4) with bimodal FV distribution (beta (0.1,0.1) ×0.04+0.03, Case B) (b). The systems A-0 or B-0 with randomly uniform or bimodal FV spatial distribution are also shown in (a) or (b), respectively. (c)-(d) The initial spatial FV distributions across the systems in Case A (A-1, A-4 and A-0) and systems (B-1, B-4 and B-0) in Case B, respectively.

and $\frac{\partial \bar{v}_f}{\partial t} = v^* f \exp\left(-\frac{\alpha v^*}{\bar{v}_f}\right) \exp\left(-\frac{\Delta G^m}{k_B T}\right)\left[\frac{2\alpha k_B T}{\bar{v}_v S}\left(\cosh\left(\frac{\tau\Omega}{2\alpha k_B T}\right) - 1\right) - \frac{1}{n_D} + \kappa\nabla^2\bar{v}_f\right]$, where $\bar{v}_f$ is the mean free volume, α is a geometrical factor close to 1, v^* is the hard-sphere volume of the atom, k_B is the Boltzmann constant, Ω is the atomic volume, τ is the equivalent shear stress, ΔG^m is the activation energy, f is the frequency of atomic vibration, T is the temperature, n_D is the number of atomic jumps needed to annihilating a free volume equal to v^* which ranges between 3 and 10 and $S = \frac{E}{3(1-\mu)}$, where E is Young's modulus and μ is the Poisson ratio and κ is a free volume gradient coefficient. By solving the equations of the strain and stress and FV change under a given externally applied strain, we can obtain the mechanical properties of the multilayered MG composites containing various FV-gradient interfaces. In particular, a material-related parameter pertaining to the constitutive models, i.e. $D^{ep}_{ijkl} = \partial\Delta\sigma_{ij}/\partial\Delta\varepsilon_{kl}$ is implemented in the ABAQUS finite element software through a UMAT subroutine [21–24,36–38]. The material properties of bulk $Zr_{41.25}Ti_{13.75}Ni_{10}Cu_{12.5}Be_{22.5}$ MG are used. The model systems have 30000 regular elements with a length of 0.1 μm and the periodic boundary conditions (PBCs). Plane strain tensile loadings are applied with an effective strain rate of 0.1/s. Compared to the real samples, our samples used in the FEM modelling are still small. One of the consequences is that once a shear band forms and extends to a certain length, it can traverse the sample and cause failure. The application of the PBC is primarily for avoiding early failure in the small system during simulations, so we can see the formation and the evolution of the shear bands. The PBC could introduce artificial results in the calculation, such as the extended plastic regime, which would not be there if the local shear is not repeatedly carried out in the sample with the PBCs. However, we can identify these artefacts and exclude them from our results.

Here, we identify two typical cases of initial statistical distribution of FVs with their heterogeneities. Case A: the FV distributions are drawn from the random statistical distribution, as shown in A-1-A4 in Figure 1a; Case B: the bimodal distribution of FVs is shown in B1-B4 in Figure 1b. Figure 1a and 1b show the systems with 1, 2, 5 and 10 layers that have a random or bimodal FV statistical distribution, respectively. In Cases A and B, the reference systems with uniform spatial distribution of FVs are denoted as A-0 and B-0, respectively. As shown in Figure 1c and 1d, the initial spatial FV distributions and gradients across the systems A-1 and B-1, A-4 and B-4, A-0 and B-0 are compared. For the each multilayered systems, each layer has a

different FV density, and the interface is the transition region from which the gradient is defined as the difference in the FV densities in the adjacent regions divided by the width of the interface. Therefore, the thinner the interface is, the more the number of interfaces and the larger the interface gradient. For the systems in Case A, the maximum FV gradients are as follows: 0.0083 μm^{-1} for one layer, 0.01704 μm^{-1} for two layers, 0.03981 μm^{-1} for five layers and 0.08233 μm^{-1} for ten layers. For the systems in Case B, the maximum FV gradients are as follows: 0.04377 μm^{-1} for one layer, 0.08456 μm^{-1} for two layers, 0.1571 μm^{-1} for five layers and 0.1933 μm^{-1} for ten layers. The gradients in these cases are constrained by the FV statistical distributions and the number of elements used in this work, so cases A and B do not have exactly the same gradient values for the interface with the same number of layers. The same gradient can be generated in the two cases if we increase the number of elements used in the FEM. Nevertheless, with the slight difference in the current samples with 30000 mesh points, we can still extract the general trends from the gradients and their influences.

3. Results

The tensile stress–strain relations of the multilayered composites are shown in Figure 2. One can see that *the multilayered MG composites all exhibit enhanced plasticity and strength with decreasing layer width, or increasing number of layers*. For case A (Figure 2a), the peak stresses decrease only slightly, and the yield stresses remain unchanged with the decreasing interface thickness. Compared with system A-0 with uniformly distributed FVs, system A-4 with ten layers exhibits the maximum stress increased by 20.0% and the yield stress by about 10.57%. The results show that the multilayered gradient interface architecture provides additional support for enhancing mechanical properties that have been achieved through tuning the monolithic MG compositions. In the following, we get into more details for case B with a bimodal FV distribution that shows more dramatic effects in strengthening and toughening.

The tensile stress–strain relations of systems in case B, shown in Figure 2b, indicate that the maximum stress of system B-4 with 10 layers increases by nearly 21% from that of system B-1 with one layer. The strain corresponding to the peak stress of 2.917 GPa in system B-4 is 5.537%, which exceeds the strain (4.149%) at the peak stress of 2.38 GPa of system B-1. As we reported previously, for case B with bimodal FV distribution, there exists an apparent 'work hardening' beyond the yield point. Here for the multilayers, we found that the maximum stress increases further with increasing number of layers, while the yield stress and the secondary work hardening modulus, the slope of the stress–strain curves beyond the yield point, remain relatively unchanged. Compared to system B-0, which has no FV gradient, the property enhancement is even more remarkable: the maximum stress, the secondary work hardening modulus and the toughness of the layered composites increase more than twice. As compared to our early work with only one FV gradient interface [23], the enhancement in strength and toughness in the multilayered composites indicates the existence of new deformation mechanisms in the multilayered MG composites originating not only from the *gradient effect* but also from the *size effect* of layer width.

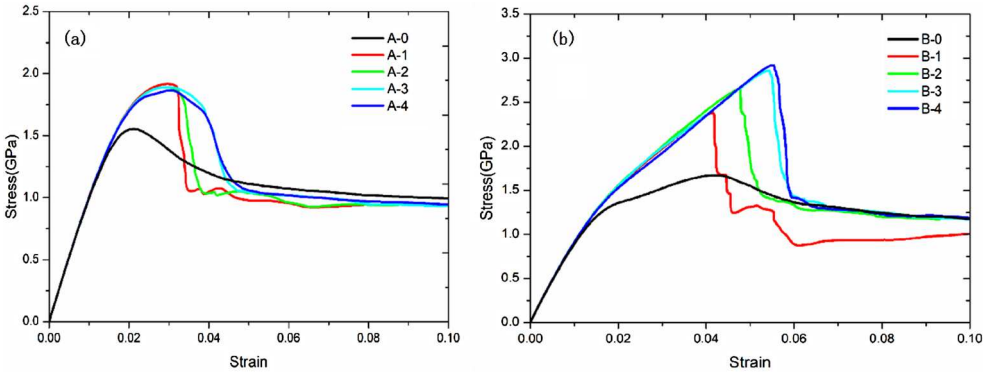

Figure 2. The stress-strain relations for systems in Case A (a) and Case B (b) with different numbers of layers. These for systems A-0 or B-0 with spatially random distribution are also shown in (a) and (b), respectively.

The size effects can be seen from the plots of the mechanical properties versus the layer width in Figure 3, which includes the maximum stress, fracture stress, flow stress, yield stress and their corresponding strains and the toughness or mechanical energy. In the plots, the fracture stress is defined as the midpoint between the maximum and the flow stresses in the plastic region [21–23]. The yield stress is determined using the 0.2% strain offset method. The change of toughness with an increasing number of layers can be quantitatively determined by calculating the area (mechanical energy per unit volume) under the stress–strain curve up to the fracture strain.

For the systems in case A with a random FV distribution (Figure 3a), the yield stress, fracture stress and peak stress decrease slightly as the layer width decreases (for systems A-1 to A-4). The strain at the peak

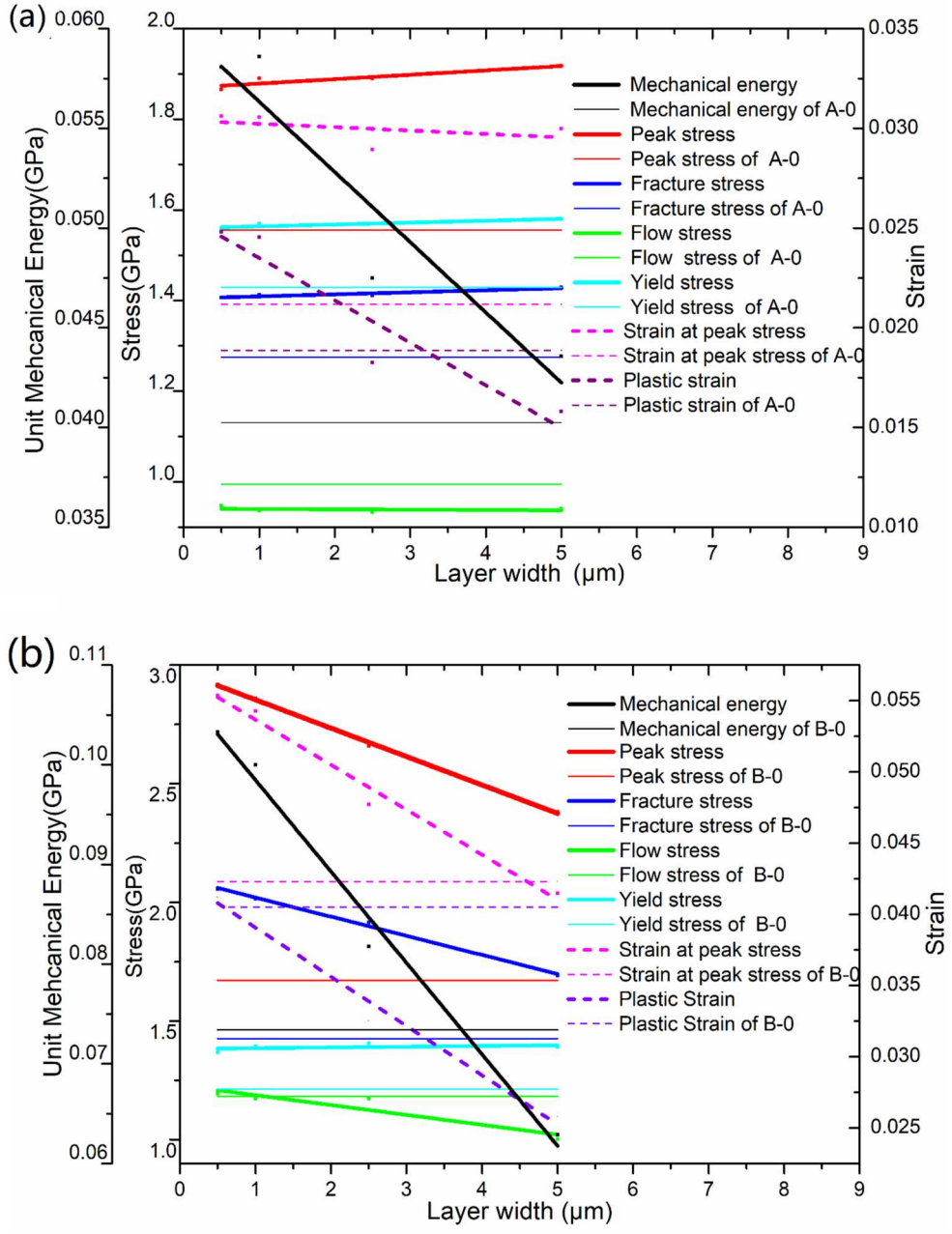

Figure 3. The maximum stress (red line), fracture stress (blue line), flow stress (green line), yield stress (cyan line), strain corresponding the peak stress (magenta dashed line), plastic strain (violet dashed line) and unit mechanical energy (black line) versus the layer width in multilayer MG composites with uniform statistical distribution (systems A-1, A-2, A-3 and A-4) (a) and bimodal statistical distribution (systems B-1, B-2, B-3 and B-4) (b). For comparison, the results of the system (A-0 or B-0) with spatially random uniform FV distribution are plotted. The lines are drawn by linear fitting.

stress and plastic strain, and especially the mechanical energy, increases as the layer width decreases. Compared to the system A-0 with randomly distributed FVs, however, the plastic strains of systems A-1 and A-2 decrease only slightly.

For the systems in case B with a bimodal FV distribution (Figure 3b), the fracture stress and peak stress increase as the layer width decreases (for systems B-1 to B-4). The yield stresses change only slightly and almost remain constant, meaning that the multilayer does not alter the yielding mechanisms of the thin MG layers. However, the strains corresponding to the peak stress, plastic strain and the mechanical energies of the systems increase significantly with decreasing layer width. For instance, the mechanical energy (0.103 GPa) of system B-4 increases with decreasing layer width, which is much larger than that of system B-1 (0.0629 GPa) and monolithic system B-0 (0.0734 GPa). The multilayered MG composites with bimodal FV distributions are, in general, becoming stronger and tougher simultaneously at a smaller layer width. These results show that the statistical FV distribution is a big factor in influencing the gradient interface effect: For the random distribution, the strength does not change much in the layered composites while the plasticity increases. For the bimodal distribution, both are enhanced.

To investigate the deformation mechanism of multilayered MG composites, the spatial FV distributions, strain and stress of the systems at different applied strain states are examined to observe the behaviours of local shear. Here we use system B as an example for its more dramatic improvement in mechanical properties. Figure 4a shows the initial state of system B-3 under tension. We use B-3 as an example to show here because other systems' layers are too thin for clear visualization.

First, we see the *preferential initiation of local shears in higher FV or softer layers*. During the deformation process, the regions with lower FV concentrations, i.e. the stronger regions, have higher local stresses. However, the regions with higher FV concentrations, i.e. the weaker regions, are deformed, resulting in a decrease in the secondary work hardening modulus of the system. In the regions with high FV

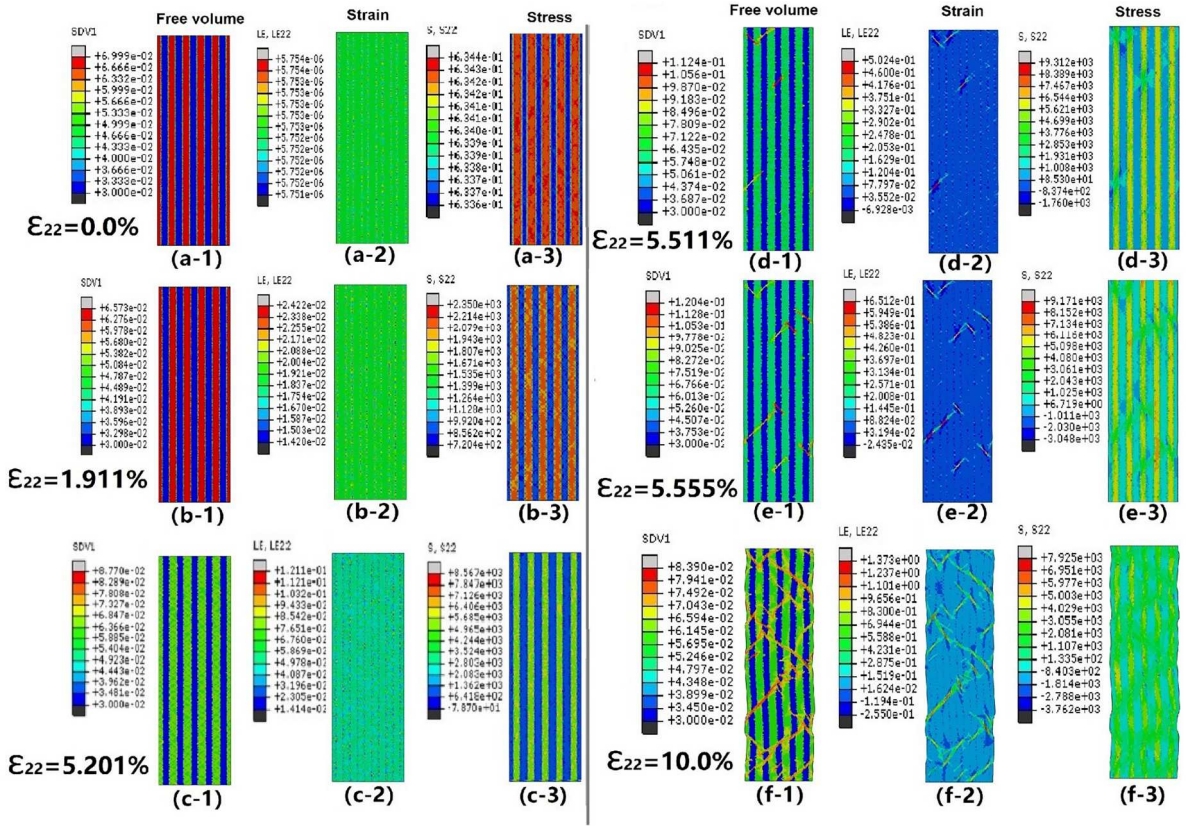

Figure 4. The contour plots of local FV (left panel), strain (middle panel) and stress (right panel) of system B-3 at six representative strains. The colour scheme is such that the lighter or warmer the colour, the higher the amplitude of the corresponding physical quantity it represents, which is also quantitatively shown in the colour bars.

concentrations, the localized *shear-banding* regions also start to form at lower applied strains. Secondly, there is a *size effect*: The narrower the region with high FV concentration, the smaller or shorter, the localized zones of shear banding. The width of the layer sets a limit for the length of the shear bands. Thirdly, all highly localized zones of *shear are contained by the FV-gradient interfaces*. Compared with those of system B-1 reported in Ref. [23], the stress distributions of systems B-3 with 5 layers are more spread or less concentrated, due largely to the presence of the multiple gradient interfaces. The shear stress around the interfaces exhibits high local values inside the regions with low FV concentrations after further deformation, as shown in Figure 4b. When the stress is lower than the peak stress in the low FV zone, those localized shear regions at the multiple FV-gradient interfaces become embryos of SBs, as shown in Figure 4c. The embryos of SBs start to extend towards the low FV zones as the stresses become high enough. The local stress at the interfaces is released as the SBs penetrate through the low FV regions of the interface, as illustrated in Figure 4d. However, FVs and strain within the SBs are elevated as a result. As the SB propagates, it will traverse the high FV zones faster and reach the next FV-gradient interface. In the next low FV regions/layers, the SB restore the mechanical energy to create higher local stress until the SB propagates again. *The more layers in the systems, the more frequent occurrence of stress release as the SBs are stopped while passing the interfaces.* Once a main SB forms and crosses the sections of the systems, the peak stress is reached, and along the same SBs, the local strain increases, as shown in Figure 4e. Under further deformation, more SBs break through the interfaces, and some new mature SBs cut through the system while those formed and broken through the multiple FV-gradient interfaces continue to deform along their paths, as shown in Figure 4f. The results in Figure 4 show that multilayered MG composites (for both case A and B) achieve higher toughness or plasticity by blocking the extension of the multiple, short, local shear zones or bands through the FV gradient interfaces to the harder layers with low FV densities.

4. Conclusions

We show that the multilayer architecture of MG composites can achieve simultaneous strengthening and toughening. First, the *gradient interface* helps in reducing the stress concentration at the interfaces. Second, the layer width functions in two different ways. One is to limit the length or *size* of the local shear regions or bands so they cannot reach maturity to cause catastrophic failure, and the second is that the increase in the number of interfaces increases the *probability* of blocking the extending or propagating shear zones or bands formed in the softer layer. The third is the *statistical FV distribution*. The bimodal FV distribution is much effective than the random or uniform distribution in enhancing plasticity and strength because of the intrinsic heterogeneity in the former. The combined effects of the above factors lead to the superior capability to enhance toughness and plasticity in MGs. We hope that the cocktail effects revealed from this theoretical work would shed new light on designing ductile and toughened MGs for their practical applications.

Disclosure statement

No potential conflict of interest was reported by the author(s).

Funding

The work is supported by the National Thousand Talents Program of China. Y.W. Wang thanks the Fundamental Research Funds for the Central Universities [grant numbers FRF-TP-20-028A1 and FRF-BD-23-02] and the Fundamental Research Funds for the Central Universities and the Youth Teacher International Exchange & Growth Program (QNXM20210044). G. P. Zheng thanks the financial support provided by the Research Grants Council of Hong Kong Special Administrative Region, China under the grant number 15233823.

Author contributions

Yongwei Wang: Writing – review & editing, Writing – original draft, Investigation, Formal analysis, Data curation, Funding acquisition. Guang-ping Zheng: Writing – review & editing, Writing – original draft, Investigation, Formal analysis, Data curation. Mo Li: Writing – review & editing, Validation, Supervision, Resources, Project administration, Methodology, Investigation, Formal analysis, Conceptualization.

Data availability statement

Data used in the work and during the simulation are available upon proper request.

ORCID

Mo Li http://orcid.org/0000-0002-6800-8776

References

[1] W.I. Klement, R.H. Willens, and P. Duwez, Nature 187 (1960), pp. 869–870.
[2] A.L. Greer, Mater. Today 12 (2009), pp. 14–22.
[3] G. Kumar, D. Rector, and R.D. Conner, J. Schroers 57 (2009), pp. 3572.
[4] S. Scudino, B. Jerliu, and S. Pauly, Scr. Mater 65 (2011), pp. 815–818.
[5] M.D. Demetriou, M.E. Launey, G. Garrett, G.P. Schramm, D.C. Hofmann, W.L. Johnson, and R.O. Ritchie, Nature Mater. 10 (2011), pp. 123–128.
[6] Q. He, J.K. Shang, E. Ma, and J. Xu, Acta Mater. 60 (2012), pp. 4940–4949.
[7] H. Choi-Yima, and W.L. Johnson, Appl. Phys. Lett. 71 (1997), pp. 3808–3810.
[8] R.D. Conner, R.B. Dandliker, and W.L. Johnson, Acta Mater. 46 (1998), pp. 6089–6102.
[9] C.P. Kim, R. Busch, A. Masuhr, H. Choi-Yim, and W.L. Johnson, Appl. Phys. Lett. 79 (2001), pp. 1456–1458.
[10] D.C. Hofmann, J.Y. Suh, A. Wiest, G. Duan, M.L. Lind, M.D. Demetriou, and W.L. Johnson, Nature 451 (2008), pp. 1085–1089.
[11] C.C. Hays, C.P. Kim, and W.L. Johnson, Phys. Rev. Lett. 84 (2000), pp. 2901–2904.
[12] H.F. Zhang, H. Li, A.M. Wang, H.M. Fu, B.Z. Ding, and Z.Q. Hu, Intermetallics 17 (2009), pp. 1070–1077.
[13] J. Das, M.B. Tang, K.B. Kim, R. Theissmann, F. Baier, W.H. Wang, and J. Eckert, Phys. Rev. Lett 94 (2005), pp. 205501.
[14] D.C. Hofmann, J. Mater. 2013 (2013), pp. 1–8.
[15] Y.F. Sun, B.C. Wei, Y.R. Wang, W.H. Li, T.L. Cheung, and C.H. Shek, Appl. Phys. Lett 87 (2005), pp. 051905.
[16] S. Pauly, J. Das, a.J. Bednarcik, N. Mattern, K.B. Kim, D.H. Kimd, and J. Eckert, Scr. Mater 60 (2009), pp. 431–434.
[17] F. Spaepen, Acta Metall. 25 (1977), pp. 407–415.
[18] A. Argon, Acta Metall. 27 (1979), pp. 47–58.
[19] Y. Wu, D.Q. Zhou, W.L. Song, H. Wang, Z.Y. Zhang, D. Ma, X.L. Wang, and Z.P. Lu, Phys. Rev. Lett 109 (2012), pp. 245506.
[20] D.C. Hofmann, Science 329 (2010), pp. 1294–1295.
[21] Y.W. Wang, M. Li, and J.W. Xu, Scr. Mater. 113 (2016), pp. 10–13.
[22] Y.W. Wang, M. Li, and J.W. Xu, Scr. Mater. 135 (2017), pp. 41–45.
[23] Y.W. Wang, M. Li, and J.W. Xu, Scr. Mater. 130 (2017), pp. 12–16.
[24] Y.W. Wang, H. Gleiter, and M. Li, MRS Bull. 48 (2023), pp. 56–67.
[25] J.W. Hutchingson, and V. Tvergaard, Int. J. Solids. Struct 17 (1981), pp. 451–470.
[26] S.Y. Kuan, H.S. Chou, M.C. Liu, X.H. Du, and J.C. Huang, Intermetallics 18 (2010), pp. 2453–2457.
[27] J. Ma, K.C. Chan, L. Xia, S.H. Chen, F.F. Wu, W.H. Li, and W.H. Wang, Mat. Sci. & Eng. A 587 (2013), pp. 240–243.
[28] C. Zhong, H. Zhang, Q.P. Cao, X.D. Wang, D.X. Zhang, J.W. Hu, P.K. Liaw, and J.Z. Jiang, J. Alloy. Comp 678 (2016), pp. 410–420.
[29] A. S´aenz-Trevizo, and A.M. Hodge, Nanotechnology 31 (2020), pp. 292002.
[30] K.P. Marimuthu, G. Han, and H. Lee, J. Non-Cryst. Solids 601 (2023), pp. 122047.
[31] X. Li, G. Li, J. Ma, Y. Cao, Y. Xu, and W. Ming, J. Manuf. Process. 117 (2024), pp. 244–277.
[32] S. Sohrabi, J. Fu, L. Li, Y. Zhang, X. Li, F. Sun, J. Ma, and W.H. Wang, Prog. Mater. Sci. 144 (2024), pp. 101283.
[33] Z.Q. Chen, M.C. Li, J.S. Cao, F.C. Li, S.W. Guo, B.A. Sun, H.B. Ke, and W.H. Wang, J. Mater. Sci. Technol 99 (2022), pp. 178–183.
[34] J.Y. Kim, D. Jang, and J.R. Greer, Adv. Funct. Mater. 21 (2011), pp. 4550–4554.
[35] Y. Wang, J. Li, A.V. Hamza, and T.W. Barbee Jr, P. Natl. Acad. Sci. USA. 104 (2007), pp. 11155–11160.
[36] Y.F. Gao, Modell. Simul. Mater. Sci. Eng. 14 (2006), pp. 1329–1345.
[37] M. Zhao, and M. Li, J. Mater. Res 24 (2009), pp. 2688–2696.
[38] M. Zhao, and M. Li, Met 2 (2012), pp. 488–507.